CW HF Chemical Laser Flow Diagnostic Measurements

ROBERT L. VARWIG* AND MUNSON A. KWOK*
The Aerospace Corporation, El Segundo, Calif.

Knowledge of local fluid dynamic properties in the flowfield of a continuous supersonic diffusion HF chemical laser is required to characterize its performance. The application of techniques for measuring local pressure and pitot pressure is described with modifications required for the hostile fluorine environment. Spectroscopic measurements of static temperature and relative concentration of HF(1) and HF(2) in the reacting fluorine-hydrogen flow then permit the deduction of crucial local flow properties in the laser medium, such as the mass density. In this report, measurements of the distribution of pitot and static pressure, static temperature, mass density, Mach number, and jet velocity are presented and the limitations in the measurements discussed. The measured concentration ratio [HF(2)]/[HF(1)] reflects the nature of the gain zone.

Nomenclature

$P(\omega_{ul}; v_u, J_u)$ = power from specific vibrational-rotational transition from the upper (u) energy level to the lower (l)
J_u = rotational quantum number
v_u = vibrational quantum number
ω_{ul} = frequency of transition (cm^{-1})
A_{ul} = Einstein A coefficient for isotropic radiation
η_0 = optical losses
Ω_0 = solid angle subtended by the optical system at the flowfield
τ = optical volume
$\bar{N}(v_u)$ = vibrational number density averaged over T
$E(v_u, J_u)$ = rotational energy level
T_R = rotational temperature (°K)
$Q(v_u, T_R)$ = rotational partition function
h = Planck's constant
k = Boltzmann's constant
c = speed of light

I. Introduction

LOCAL fluid flow properties in the supersonic freejets of a continuous-wave HF diffusion chemical laser[1-6] are of interest because they define the nature of the lasing medium. For example, the local species and gas density variations, which can be related to index-of-refraction variations, can determine the types and quality of transverse modes generated and the general optical properties of the medium. The HF(v) species can, moreover, map the gain zone. Consequently, an effort has been made to measure these or related flow properties in a given laser flowfield.

A complete characterization of a reacting flowfield requires local determinations of static pressure, static temperature, gas velocity, and species concentrations. The species concentrations must be known to provide calculations for the molecular weight W of the gas as well as the ratio of specific heats γ. The concentrations of majority species, diluent He and fuel H_2, can be estimated from flow rate measurements and, since these lasers typically run diluent rich ([HE]/[F] > 5), γ is an insensitive parameter and can be estimated by considering the gas to consist mainly of a He-H_2 mixture. As will be shown, the variation in W is also satisfactorily small for the flow conditions usually obtained. Thus, from a measurement of pitot and static pressure and the Rayleigh formula, an estimate of Mach number M can be made. When T is measured, the local frozen sound speed can be computed and, from that, the gas velocity. The all-important gas density can be computed from the usual gas law for given p, W, and T.

It became the objective of this study, therefore, to examine the application of traditional means for measuring the static and pitot pressures and the temperature in the reacting flow that constitutes the lasing medium of a diffusion chemical laser. The techniques applied are described and evaluated, and some typical results and an interpretation of the measurements for the so-called three-dimensional modular nozzle bank are presented.

Received May 22, 1973; revision received August 31, 1973. This work reflects research supported by the Air Force Weapons Laboratory, under U.S. Air Force Space and Missile Systems Organization (SAMSO) Contract F04701-73-C-0074. The authors wish to acknowledge the helpful discussions with H. Mirels, G. Emanuel, and R. R. Giedt, and the assistance of H. Bixler, T. Felker, J. Blades, and R. H. Ueunten.

Index category: Reactive Flows.

* Member of the Technical Staff, Aerophysics Laboratory. Member AIAA.

II. Test Facility and Flow Conditions

Measurements were made in the supersonic diffusion laser facility (Fig. 1) employing a three-dimensional nozzle 0.5 in. long with a throat cross section of 0.042×0.084 in. and an exit area of 0.119×0.500 in. In this facility, which has up to 27 nozzle elements, fluorine atoms are obtained from SF_6 introduced into the plenum with hot helium. Hydrogen is injected at the nozzle exits from the slits on each side of every nozzle as shown in Fig. 1. The mixing of H_2 with the fluorine nozzle flow produces the reaction $F+H_2 \rightarrow HF(v)+H$, which causes vibrationally excited HF(v) to occur. There was no laser optical cavity in place during these tests; hence, zero power conditions existed.

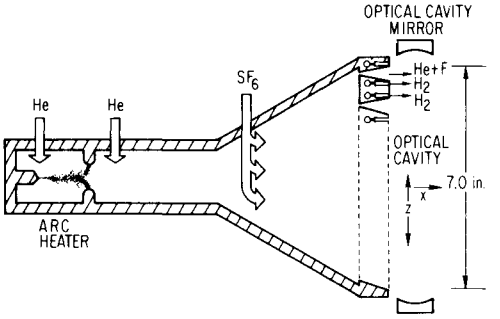

Fig. 1 Multiple grid nozzle scheme for supersonic diffusion laser.

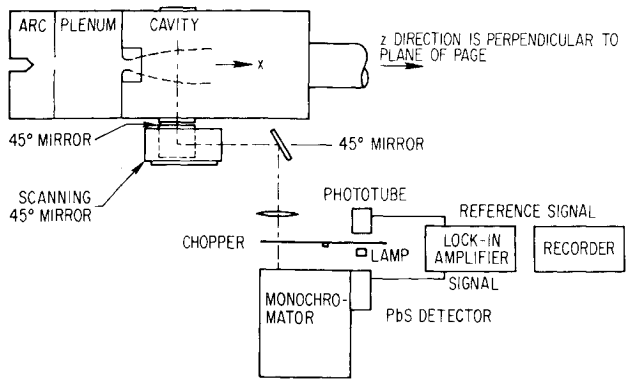

Fig. 2 Schematic for rotational temperature-measuring apparatus and HF CW laser.

For the high plenum pressures desired for these studies, respective mass flows of 8 and 7.4 g/sec of SF_6 and He were employed. The plenum pressure reached 8.5 atm, and plenum temperature ranged from 1800 to 2100°K. Using the NEST computer program developed at The Aerospace Corp.,[7] values of the average molecular weight W and the ratio of specific heats were determined for a range of temperature from 300 to 2300°K at 8.5 atm. For this range, W varied less than 9% and the variation in γ was even smaller. Assuming frozen flow in the nozzles at the plenum conditions, values of W and γ of 8 ± 0.2 g/mol and 1.55–1.58 were determined for nozzle exit flow conditions. Further downstream in the laser cavity, with 2 g/sec H_2 injected and assuming a well-mixed gas, limiting values were again computed, this time including the hydrogen fuel. From these calculations, W and γ were estimated to range from 5.6 to 6.3 g/mol and from 1.51–1.56.

III. Measurements

Pitot pressure is relatively easy to measure in ordinary noncorrosive hot gas flows in the laser cavity.[8] However, materials at high temperature are attacked by fluorine and, hence, there is the requirement to keep the probe cool. The pitot probe designed to fill this requirement consists of a wedge, the leading edge of which is 0.020 in. thick with an inlet port 0.010 in. in diameter. Hence, the spatial resolution is between 0.010 and 0.020 in. compared to the 0.119-in. width of the nozzle elements. Cooling water is circulated through the probe body, and the temperature-compensated strain gauge transducer contained in the probe for sensing pressure never approaches the temperature compensating limit of 250°F. The resonant frequency of the combination of the inlet, gauge cavity, and gauge is about 80 Hz. Hence, the probe response is fast enough to record pitot pressure while it slowly traverses the tunnel.

The static pressure model is a flat plate/wedge with the pressure inlet port, a $\frac{1}{64}$-in.-diam hole, 0.2-in. aft of the sharp leading edge. Because the probe is cooled and the Reynolds number is high, viscous induced pressure and flow deflection can be neglected.[9] The pressure signal is conducted to a U-tube manometer, filled with Meriam 104 fluid, located outside the tunnel. Since these lines are long and of small diameter, the response time of the pressure monitoring system is on the order of minutes. Hence, sweeps of the static probe are not possible. The probe must be located, the tunnel operated, and the pressure measured. Then the probe is moved to a new location, and the pressure is measured again in the next tunnel test. As a result, there was concern for the repeatability of the tunnel operation. The mass flows were identical for almost all the tests conducted, and were monitored with float-type flow meters. For the pressure measurements the plenum pressure (the only measured plenum parameter) varied from 7.5 to 8.5 atm for a range of $\pm 6\%$. Therefore, this range must be considered to be the lower limit on the uncertainty in the pressure measurement. No significant pressure variation occurred within individual tests since the 3-D nozzles have a large hydraulic diameter and resist becoming fouled by sulfur and arc debris.

Measurements of the static temperature T have been made using a spectroscopic technique involving the HF $1 \rightarrow 0$ vibrational band. The line of sight is in the thin jet (0.8 in.) or y direction. For sufficiently small optical volumes far enough downstream in the jet, the static temperature can be assumed to be uniform within the volume. Then T can be found from the relative intensity measurements of the optically thin R-branch lines $R_1(1)$ through $R_1(6)$ from

$$\ln\left[\frac{P(\omega_{ul};\, v_u, J_u)}{(2J_u+1)A_{ul}\,\omega_{ul}}\right] = \ln\left[\frac{hc}{4\pi}(\eta_0\Omega_0\tau)\frac{\bar{N}(v_u)}{Q(v_u, T_R)}\right] - \frac{hc}{kT_R}E(v_u, J_u) \tag{1}$$

The assumptions are made that rotational equilibrium exists among HF molecules and rotational-translational equilibrium is obtained. That is,

$$T \simeq T_R \tag{2}$$

The T_R can be determined by plotting $(P/2J+1)(\omega_{ul}A_{ul})$ vs $E(v_u, J_u)$ on a semilogarithm plot. The slope of the line is hc/kT_R.

The experimental arrangement is shown in Fig. 2. A spectrally scanning prism monochromator was coupled to a scanning mirror system. The moving mirrors permitted the placement of optical volume τ at a given position x and z in the flow. The downstream direction is x, and z is the direction of the cavity axis. The spatial resolution is the slit image given by a rectangle $(\Delta x)(\Delta z) = (8\text{ mm})(0.5\text{ mm})$ compared with the nozzle z dimension of 3.02 mm.

Spectral line radiation was recorded using the lock-in

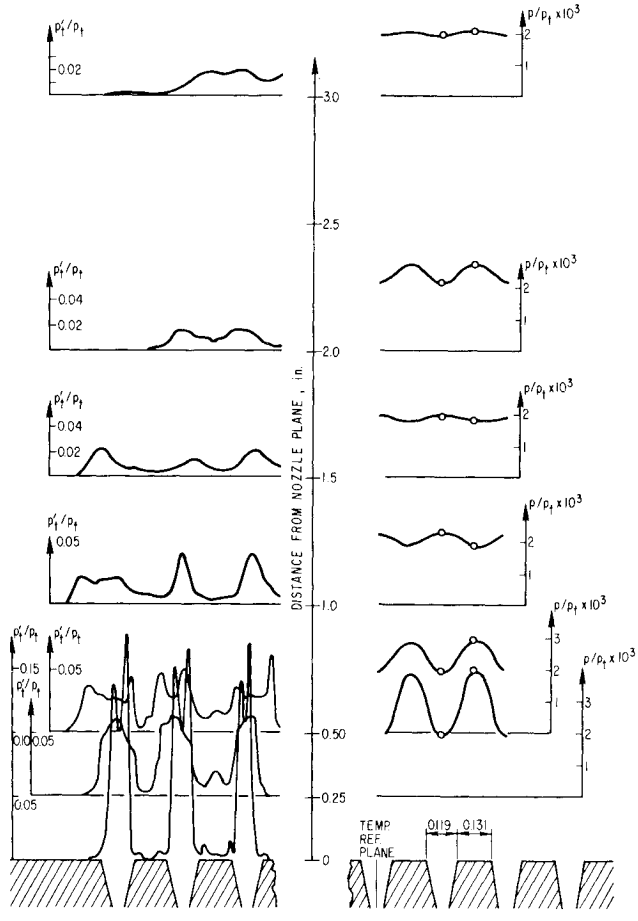

Fig. 3 Pitot and static pressure profiles of three-dimensional nozzle.

Table 1 Centerline flow properties in laser cavity downstream of 3-D nozzle

Distance from nozzle exit (in.)	p_t (atm)	T_t (°K)	$\frac{p_t'}{p_t}$	$\frac{p}{p_t}$	T (°K)	M	U (cm/sec)	ρ (g/cm^3)
								($W = 8$)
0 00	8.30	1820	0.096	0.19×10^{-2}	149[a]	5.8	2.86×10^5	1.0×10^{-5}
0.25	8.02	1850	0.062	0.20×10^{-2}		4.8		
								(W = 6)
0.50	8.43	1850	0.026	0.19×10^{-2}	400	3.1	2.9×10^5	0.29×10^{-5}
1.0	8.50	1980	0.038	0.22×10^{-2}	500	3.3	3.4×10^5	0.28×10^{-5}
1.5	8.50	1900	0.020	0.19×10^{-2}		2.6		
2.0	7.48	1760	0.015	0.21×10^{-2}	550	2.2	2.4×10^5	0.21×10^{-5}
3.0	4.76	1820	0.017	0.20×10^{-2}	600	2.4	2.7×10^5	0.11×10^{-5}

[a] Determined from plenum conditions and exit Mach number.

amplifier technique for optimum signal-to-noise ratio. The detector was photoconductive PbS with a 510-kohm load. Chopping frequency was 250 Hz. The space between the window and the jet contained a shroud that was carefully flushed with dry N_2 gas to eliminate the absorption of radiation due to recirculating ground state HF. The recording of one spectrum at a given spatial location required 70 sec. Thus, the information is highly time-averaged.

The HF $1 \rightarrow 0$ R-branch was chosen to avoid the problems of atmospheric absorption and the necessity of flushing the optical path external to the laser cavity chamber. With a little additional effort, the $2 \rightarrow 1$ $R(4)$ line cas also be recorded. The inversion ratio for HF(2) over HF(1) can be determined with the relative intensity measurements using this line with the $1 \rightarrow 0$ $R(4)$ line

$$\frac{\bar{N}(2)}{\bar{N}(1)} = \frac{P(3964; 2, 5)}{P(4143; 1, 5)} \times 5807\, e^{-(33.281/T)} \tag{3}$$

For sufficiently small $(\Delta x)(\Delta z)$, the local measurement $N(2)/N(1)$ is approximated. The $2 \rightarrow 1$ $R(4)$ line is chosen because it is a well-isolated transition, and the ratio is insensitive to T (varying by less than 7% over the range of 300–700°K). With the monochromator fixed at the two line positions, continuous scans in z were performed.

The wavelength dependence of the entire optical system was determined in a usual relative calibration using a blackbody infrared source.

Table 2 Rotational temperature and relative HF excited state number density downstream of 3-D nozzle

Distance from nozzle exit (in.)	Transverse Distance from ref. nozzle C_L(in.)	p_t (atm)	T_t (°K)	T_{ROT} °K	[HF(2)]/ [HF(1)]
0.66	0.0938	6.8	2300	452	0.93
	0.1563			379	1.0
	0.2188			399	0.93
1.0	0.0938	6.8	2300	432	0.95
	0.2188			502	0.79
	0.5438			416	0.83
2.0	0.0938	6.8	2300	586	0.89
	0.5438			562	0.66
	0.9376			570	1.0
	1.188			607	
3.0	0.0938	6.8	2300	495	0.60
	0.2188			560	0.51
	0.5438			623	0.58
3.88	0.0938	6.8	2300	595	0.43
	0.2188			590	0.42
	0.5438			564	0.43

IV. Discussion of Results

Typical pitot and static pressure profiles obtained in the laser cavity at stations from the nozzle exit to 3-in. aft are shown in Fig. 3 along with the temperature reference plane. The data are listed in Tables 1 and 2. From these measurements the density was computed based on an average molecular weight of 6. These values are plotted isometrically in Fig. 4.

Static pressure (right side of Fig. 3) is measured along the axis of nozzle 3 and in the void between nozzles 3 and 4. The pressure measured between the nozzles at stations $\frac{1}{4}$ and $\frac{1}{2}$-in. aft of the exit plane is much larger than that along the nozzle axis at these stations. This is probably due to the hydrogen injection that occurs between the nozzles as indicated in Fig. 1. At 1-in. downstream from the exit, the difference is greatly diminished. Aside from this variation close to the nozzle exit, the static pressure along the axis is within $\pm 5\%$ of 2×10^{-3} p_t, and the transverse variation is less than $\pm 15\%$. It is in this range, where variations are small, that this measurement of static pressure is most applicable.

In general, the pitot pressure (left side of Fig. 3) reflects the dynamic pressure which is maximum along the nozzle axes. At the nozzle exit plane, the flow is locally overexpanded because of the H_2 injection and the hydrogen-fluorine reaction. The flow separates upstream of the nozzle exit, and the familiar separation shock waves appear as exhibited by the sharp peaks on the sides of each nozzle pitot profile. Further downstream, the pitot pressure is affected by the wake recompression shock structure in the wake of the base region between the nozzles (e.g., the profile at the 0.50-in. station).

From the temperature measurements, one concludes first that the temperature variation is small, ranging from just under 400°K $\frac{1}{2}$ in. from the nozzle to nearly 600°K 4 in. downstream. Transverse variation, i.e., from a nozzle centerline to just in between two nozzles, is 50°–100°. Probably the most rapid change occurs within the first $\frac{1}{2}$ in. of flow since this is where most of the reaction occurs. Here the temperature must rise from the freestream value of 150° to 160°K to nearly 400°K $\frac{1}{2}$ in. aft.

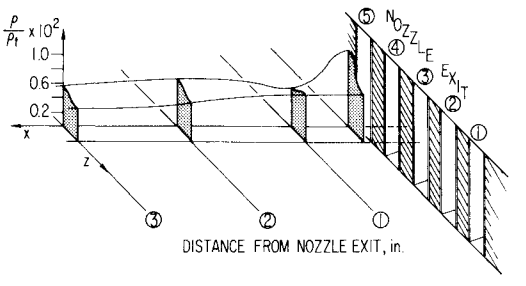

Fig. 4 Density map in laser cavity—three-dimensional modular nozzle.

From that point on, temperature increases are much more gradual.

The uncertainty in the measurement of T_R lies mainly in the measurements of spectral line power P, which occasionally fluctuated slowly $\pm 10\%$ with the monochromator set at one spectral line position. Considering the measurement of $P(\omega_{ul}; v_u, J_u)$ for seven $1 \rightarrow 0$ R-branch lines over $E(v_u, J_u)$ from 39 to 1414 cm^{-1}, the uncertainty in T_R is shown to be $\pm 7\%$ or, at the largest x, $\pm 40°K$. The uncertainty is minimized despite large temporal fluctuations because of the large number of R-branch spectra $[R_1(1)$ to $R_1(8)]$ used to determine the slope hc/KT_R. Neglecting the slow fluctuations, the signal-to-noise ratio was 100:1 for the strongest lines, and the fact that the R-branch spectra yielded such straight lines (Fig. 5) over a large J_u range indicates the absence of significant self-absorption due to HF(0) in the flame regions. Because of the high plenum pressure and the large hydraulic diameter throat, the boundary layers are much thinner than those in the 36-slit nozzle configuration.[1-6] The influence of self-absorption from HF(0) is therefore postponed to regions further downstream because the more inefficient mixing of thinner layers and higher exit static pressures tends to lead to lower local HF concentrations at small x.

In a finite optical volume τ in these flows with essentially low spatial resolution compared to the limiting dimension of the reaction region, spatial nonuniformities do exist. The spontaneous emission reflects gas dynamic conditions existing primarily within the reaction zone where HF(v) is produced. Therefore, T_R in this subregion is deduced although τ may be larger. For uniform T within τ, Eq. (1) is exact although HF(v) densities may vary greatly. For T not uniform in τ, it can be shown that an increasing systematic deviation from the straight line on the semilogarithm plot for increasing J_u would be observed, and the apparent T_R' deduced as an upper bound on T_R considered as the average temperature in τ. It can also be shown mathematically that substantial spatial variations in T must exist for small deviations in T_R' from T_R. Actual data (Fig. 5) adhere to the straight line, as previously noted, and we conclude that nonuniformity effects for given τ are not great in these studies.

The density reflects the static pressure quite closely, which is to be expected since the temperature is relatively constant over the region where the density is determined. At the $\frac{1}{2}$-in. position, the He and H_2 are probably not well mixed; therefore, calculating the density based on an average molecular weight of 6 is not satisfactory. Along the centerline of the axis, the average molecular weight could be close to 8, which reflects the plenum conditions. Between the nozzles, the preponderance of H_2 could lead to an average molecular weight closer to 2. Using these extremes, density values 1.3 times higher on the nozzle centerline and one-third as much between the nozzles are obtained.

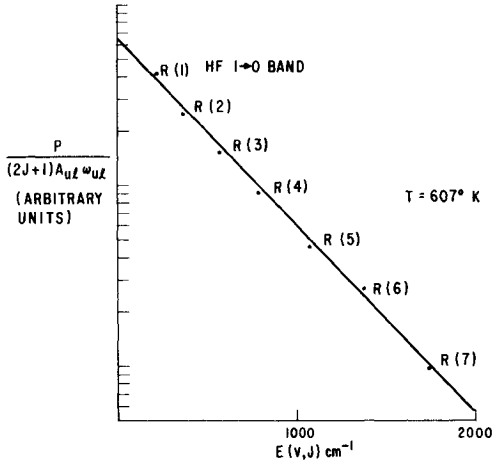

Fig. 5 Sample of typical rotational temperature determination from spectroscopic data.

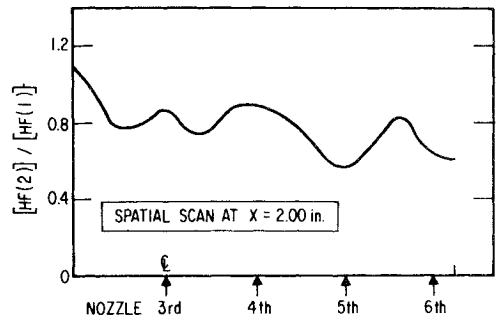

Fig. 6 $\bar{N}_2/\bar{N}_1$ vs z at $x = 2.00$ in.

At the nozzle exit, the Mach number is about 5.8. This value decreases fairly steadily to 2.5 at 3 in. downstream. The decreasing Mach number results more from increasing temperature because of heat release from the reaction than from decreasing flow speed. The flow speed changes only slightly, as indicated in Table 2.

Measurements of the ratio of number densities in zero power of HF second and first vibration levels are shown in Fig. 6. These data were obtained by setting the monochromator on a specific line and then performing a spatial scan. Considerable variation with z is observed in the quantity, and the variation with z in the line intensity from which the ratio was obtained was as much as a factor of 2. It appears that the spatial variation in number densities may be more significant than the variation of rotational temperature in this particular jet. Knowledge of the ratio, the rotational temperature, and the assumption of rotational equilibrium permits a study of spatial variation of the relative gain coefficients for the $2 \rightarrow 1$ HF band. The spectral line within the band of maximum small signal gain is seen to change across the flow. More details on such phenomena will be sought in future investigations.

V. Summary

In this study the application of techniques has been investigated for measuring pitot pressure, static pressure, and temperature to determine the properties in the reacting flowfield of a supersonic diffusion chemical HF laser. The cooled pitot probe devised measures stagnation pressure, which has a satisfactory resolution relative to nozzle dimensions. Static pressure measurements are most reliable from 1 in. aft of the nozzle exit plane where pressure variations are small. Closer to the nozzle exit, the static pressures may be influenced by the individual component flow streams. Temperature measurements are commensurate with the quality of the static pressure, and the densities determined in the flowfield have the same reliability as the static pressure and temperature. Mach number is obtained from the pitot and static pressures and has the same reliability as the static pressure. From relative HF(v) number density measurements, a considerable spatial variation in HF(v) number density was noted which deserves further investigation.

References

[1] Spencer, D. J., Jacobs, T. A., Mirels, H., and Gross, R. W. F., "Continuous-Wave Chemical Laser," *International Journal of Chemical Kinetics*, Vol. 1, Sept. 1969, pp. 493–494.

[2] Spencer, D. J., Mirels, H., Jacobs, T. A., and Gross, R. W. F., "Preliminary Performance of a CW Chemical Laser," *Applied Physics Letters*, Vol. 16, March 1970, pp. 235–237.

[3] Spencer, D. J., Mirels, H., and Jacobs, T. A., "Comparison of HF and DF Continuous Chemical Lasers: I. Power," *Applied Physics Letters*, Vol. 16, May 1970, p. 386.

[4] Kwok, M. A., Giedt, R. R., and Gross, R. W. F., "Comparison of HF and DF Continuous Chemical Lasers: II. Spectroscopy," *Applied Physics Letters*, Vol. 16, May 1970, p. 387.
[5] Spencer, D. J., Mirels, H., and Jacobs, T. A., "Initial Performance of a CW Chemical Laser," *Opto-Electron*, Vol. 2, 1970, pp. 155–160.
[6] Spencer, D. J., Mirels, H., and Durran, D. A., "Performance of CW Chemical Laser with N_2 or He Diluent," *Journal of Applied Physics*, Vol. 43, No. 3, March 1972, pp. 1151–1157.
[7] Turner, E. B., Emanuel, G., and Wilkins, R. L., "The NEST Chemistry Computer Program," TR-0059(6240-20)-1, July 1970, The Aerospace Corp., El Segundo, Calif.
[8] Varwig, R. L., "Chemical Laser Nozzle Flow Diagnostics," TR-0172(2779)-1, Feb. 1972, The Aerospace Corp., El Segundo, Calif.
[9] Hall, J. G. and Golian, T. C., "Shock Tunnel Studies of Hypersonic Flat Plate Air Flows," AD-1052-A-10, Dec. 1960, Cornell Aeronautical Lab., Buffalo, N.Y.

FEBRUARY 1974 AIAA JOURNAL VOL. 12, NO. 2

Role of Binders in Solid Propellant Combustion

N. S. COHEN,* R. W. FLEMING,* AND R. L. DERR†
Lockheed Propulsion Company, Redlands, Calif.

This paper describes a preliminary investigation into the effects of inert binder properties on composite solid propellant burning rate. Surface pyrolysis data were obtained for many polymers over a wide range of conditions, using a focused radiation source. These data were used to extract kinetics constants from Arrhenius plots, and heat of decomposition from an energy balance. Motion pictures were taken of the pyrolyzing surfaces, and gas samples were extracted for spectrometric analysis. Pyrolysis kinetics varied between the polymers, but were found to be independent of nitrogen pressure, the presence of ammonium perchlorate or catalysts in the sample, and their combinations. All of the polymers exhibited molten, boiling surfaces mingled with char, to varying degrees; the low activation energies measured may be associated with the boiling, or with a weak-link decomposition mechanism. Relevant data were input into the Derr-Beckstead-Price combustion model in order to associate binder properties with known effects on burning rate in simple propellants. Although the effects were predictable, they stemmed from properties other than pyrolysis kinetics. It appears that the role of binder lies in its contributions to controlling gas phase processes, and not in surface pyrolysis properties.

Introduction

COMPARED to the considerable effort that has been devoted to improved understanding of the role of ammonium perchlorate in solid propellant combustion, little attention has been given the binder.[1] The rationale for this difference in emphasis arises from the use of oxidizer to control propellant combustion characteristics, whereas the binder fulfills an essentially different role. However, as sophistication of combustion modeling and combustion tailoring has advanced, the need for additional attention to the role of the binder in the combustion process has become recognized.

Hypotheses concerning the role of binder in solid propellant combustion may encompass a variety of conceivable physical and chemical processes. Physical processes include the binder as inert interstitial spacing between oxidizer particles to impede the combustion front on the local microscopic scale; surface melting that would result in physical interference with oxidizer processes and thereby the ability of the oxidizer to react with binder or otherwise manifest itself; heat transfer and phase changes; diffusion of binder decomposition products in the gas phase; and processes that have a feedback effect upon the physical geometry of the combustion zone. Chemical processes include thermal and/or oxidative degradation of the polymer; and reactions between the products of binder decomposition with those of oxidizer decomposition or combustion in various regions of the gas phase or in stages. The kinetics and energetics of these processes serve to quantify the burning rate of the propellant and the various details that relate to burning rate (e.g., surface temperatures, flame heights, whether the oxidizer particles are recessed into the binder surface or protrude above it). These processes actually contribute to a total picture, and must be considered in that context. The extraction of an individual hypothesis concerning the role of binder, with nothing more, has not yet provided a reconciliation of propellant combustion behavior with the binder as a variable.

Combustion models of the type developed by Hermance[2] and by Derr, Beckstead, and Price[3] have attempted to include most of these processes in a reasonable manner, to the extent justified by experimental knowledge but within the limits of tractability, so that they may be analytically studied individually and coupled. However, many of the essential parameters affected by the binder have been quantified by assumptions based on limited data of questionable relevance. Typical criticisms are that the information used was acquired at heating rates many orders of magnitude below the rates that occur in the combustion zone, or under conditions of otherwise limited applicability to propellant combustion, or for polymers that are of limited or no interest to the propellant industry. Several recent programs have moved to overcome these criticisms[4–9]; however, they are limited in scope with reference to the acquisition of model input parameters. Accordingly, one purpose of this work was to expand

Presented as Paper 72-1121 at the AIAA/SAE 8th Joint Propulsion Specialists Conference, New Orleans, La., November 29–December 1, 1972; submitted April 10, 1973; revision received October 5, 1973. This work was performed under Contract F04611-71-C-0061, Air Force Rocket Propulsion Laboratory, Edwards, Calif.
Index categories: Combustion in Heterogeneous Media; Fuels and Propellants, Properties of.
* Technical Specialists, Engineering Research Department.
† Supervisor, Combustion Section, Engineering Research Department. Member AIAA.